IOP Publishing Journal of Physics: Condensed Matter
J. Phys.: Condens. Matter **32** (2020) 225803 (5pp) https://doi.org/10.1088/1361-648X/ab7578

Ultrafast magnetization dynamics in the vicinity of spin reorientation transition in $TbCo_2$/FeCo heterostructures

Mikhail Gaponov[1], Sergei Ovcharenko[1], Alexey Klimov[1], Nicolas Tiercelin[2], Philippe Pernod[2], Elena Mishina[1], Nikita Ilyin[1], Alexandr Sigov[1] and Vladimir Preobrazhensky[3]

[1] MIREA—Russian Technological University 'RTU MIREA', 119454 Moscow, Russia
[2] Univ. Lille, CNRS, Centrale Lille, ISEN, Univ. Valenciennes, UMR 8520—IEMN, F-59000 Lille, France
[3] Prokhorov General Physics Institute of RAS, ul. Vavilova 38, 119991 Moscow, Russia

E-mail: mishina_elena57@mail.ru

Received 1 November 2019, revised 14 January 2020
Accepted for publication 12 February 2020
Published 5 March 2020

Abstract

The magnetic moment dynamics excited by 35 fs laser pulses in $TbCo_2$/FeCo heterostructure is experimentally investigated by pump-probe technique. The studies are carried out in two typical geometries with magnetizing field perpendicular and along to the easy magnetization axis. In the 'easy axis' orientation, high-frequency oscillations of magnetic moments odd with respect to the sign of the magnetizing field are observed using the magneto-optical Kerr effect. In the perpendicular 'hard axis' orientation corresponding to the spin reorientation phase, the experiment shows oscillations that are even with respect to the field. The maximum angle of Kerr rotation as a function of the magnetizing field strength depicts a specific hysteretic loop that reveals ultrafast optical control of uniaxial magnetic anisotropy originally induced during deposition of the heterostructure in a DC magnetic field. The results provide new ways of ultrafast control of magnetic states in exchange coupled intermetallic heterostructures designed for spintronic applications.

Keywords: magnetic heterostructures, ultrafast demagnetization, optical control of magnetization, femtosecond laser, pump induced effects

(Some figures may appear in colour only in the online journal)

1. Introduction

Efficient control of magnetization is a key requirement to high performance of magnetic memory and other advanced spintronic devices [1]. Femtosecond optical pulses are proved to be a tool for ultrafast magnetization control [2, 3]. Mostly, magnetic thin films with strong perpendicular magnetic anisotropy are studied to simultaneously satisfy the requirements for storage density and thermal stability [4].

At the same time, spin dynamics induced by femtosecond laser pulses in structures with in-plane anisotropy is of a particular interest for studies of ultrafast processes in the vicinity of spin reorientation transitions (SRT). The proximity to the magnetic phase transition of order-order type increases the spin system sensitivity to external impacts and creates favorable conditions for observation of optically induced phenomena. Usually either materials with natural SRT (induced by temperature changing) [5–7] or heterostructures based on them [8, 9] are studied.

In recent years the interest in spin reorientation dynamics increased due to the prospects of stress-mediated magnetoelectric memory cells (MELRAM) [10–12]. Rare-earth intermetallic heterostructures with giant magnetostriction like $TbCo_2$/FeCo are considered as candidates for MELRAM application. Their magnetic system consists of exchange-coupled ferromagnetic and ferrimagnetic nanolayers with uniaxial magnetic anisotropy artificially induced during the layers deposition in a DC magnetic field. The technology

allows one to vary magnetic and magneto-elastic parameters of such structures in a wide range [13]. An example of the complex nanostructure with technologically determined magnetic parameters is of a basic interest for studying ultrafast dynamics in spin systems. In this work, we studied the magneto-optical response of intermetallic rare-earth multilayer nanostructure to a 35 femtosecond optical pulse. Special attention is paid on conditions of spin reorientation where competition between Zeeman interaction and uniaxial anisotropy takes place.

2. Methods

In this work, we studied the magneto-optical response of intermetallic rare-earth multilayer nanostructure to a 35 femtosecond optical pulse. The experiments were carried out on the sample consisting of a stack composed of 14 alternating exchange-coupled layers (TbCo2)—2.4 nm and (FeCo)—1.5 nm on a silicon oxide substrate (the same sample family that was first reported in [14]). This nanostructured film was deposited onto the silicon by radio frequency (RF) sputtering using a rotary turn table in a Leybold Z550 equipment, while applying a DC magnetic field on the substrate in order to induce uniaxial magnetic anisotropy in the layer plane [15]. The base vacuum in the chamber prior sputtering was 3×10^{-7} mbars. During the sputtering operation, a pure Argon flow is maintained with a flow rate adjusted to reach the desired deposition pressure; in order to obtain the correct stoichiometry from the composite targets, Ar pressure is 10^{-3} mbars with a 250 Watts RF power for the TbCo alloy, and 2×10^{-3} mbars with a 440 Watts for FeCo. The thickness is adjusted with the angular speed of the rotary table. This scheme allows for precise and reproductible layer thicknesses. When the number of layers is from 10 to 20, the properties of the sample do not noticeably change.

Magnetic properties of the samples were tested for in-plane orientations of magnetic field using a vibration magnetometer ADE EV9 with resolution of $1 \div 5$ μemu. Magnetization curves (figure 1(a)) demonstrate unambiguously strong in-plane anisotropy. The anisotropy field strength defined as saturation field for 'hard axis' geometry was found as $H_a = 8$ kOe. Saturation magnetization is equal to $B_s = 5.7$ kG. For the direction of magnetization along the 'easy axis', coercive field is determined as $H_c = 0.38$ kOe.

For optical excitation of the spin system, an amplified titanium-sapphire femtosecond laser was used. At the output of the amplifier, the radiation had the following parameters: a wavelength of 800 nm, a repetition rate of 3 kHz, a pulse duration of 35 fs. The output beam was split into the excitation (pump) and the probe channels. The energy density on the sample surface in the pump and in the probe pulses was about 0.85 mJ cm^{-2} and 0.085 mJ cm^{-2}, respectively. The spot diameter of both the pump and probe is 200 μm. Angles of incidence of the pump and probe beams onto the sample surface were 20° and 45° respectively as it is shown in figure 1(b). The sample was placed between the poles of an electromagnet, which allowed application of magnetic field up to 5.5 kG in the optical plane of incidence at 45 degrees to the film plane. The polarization of both the pump and probe beams was linear, the electric field vector lay in the joint plane of incidence (p-polarization). Orientation of magnetic field was fixed in the same plane. By rotating the sample around the normal to the surface, we directed the easy magnetization axis of the structures either along the joint plane of incidence ('easy axis' geometry) or perpendicular to that plane and thus perpendicular to the magnetic field ('hard axis' geometry). Only 'easy axis' geometry is shown on the figure 1(b). Two types of experiments were carried out: (I) the delay time was changed for a fixed magnetic field; (II) at a fixed delay time, the magnetic field was changed. In this way, dynamic hysteresis loops were measured. All experiments were performed at room temperature. For detection of magnetic moment oscillations, a balanced photodiode was used, which makes it possible to detect simultaneously the angle of rotation of the polarization plane and the intensity of the reflected wave. To improve the signal-to-noise ratio, an opto-mechanical chopper was used for modulating the intensity of the pump wave in combination with a lock-in amplifier.

3. Results

Figure 2 presents excitation–relaxation temporal dependences of the polarization rotation angle when the magnetization easy axis lies in the plane of incidence ('easy axis' geometry). Under femtosecond pulse excitation, all curves start with initial spike of polarization rotation [16]. After that, total slow relaxation occurs much longer than the maximal delay time that is 800 ps in our experiments (not shown here). On the background of slow relaxation, oscillations are observed. They relax much faster than transient background relaxation takes place. Temporal dependences are odd regarding to magnetic field direction: the magnetic field reversal results in change of the rotation angle sign. Hysteresis loops are also odd respectively to the magnetic field (see figure 2(b)). Magneto-optical loops are almost rectangular. For the time range of oscillations attenuation ($t = 150$ ps), the rotation angle tends to the transitory values a little lower than for the moment correspondent to the maximum oscillations amplitude ($t = 20$ ps).

When the easy magnetization axis lies perpendicular to the plane of incidence ('hard axis' geometry), magnetic system undergoes SRT under variation of magnetic field strength [17, 18]. The spin reorientation is caused by competition between uniaxial anisotropy and Zeeman interaction of magnetic moment with an external magnetic field. When the magnetic field is stronger than the anisotropy field $H > H_a$, the magnetic moment is parallel to H (collinear phase). When $H < H_a$, the magnetic moment deviates from the magnetic field towards the easy magnetization axis (angular phase). The projection of the magnetization on the easy axis depicts a specific hysteretic loop.

Figure 3 presents excitation–relaxation temporal dependences of the polarization rotation reproducing magnetization hysteresis loop in the angular phase. Contrary to the 'easy axis' geometry, in the 'hard axis' geometry the polarization rotation loop in figure 3(a) is even. Since the anisotropy field is stronger than the applied magnetic field, the hysteresis

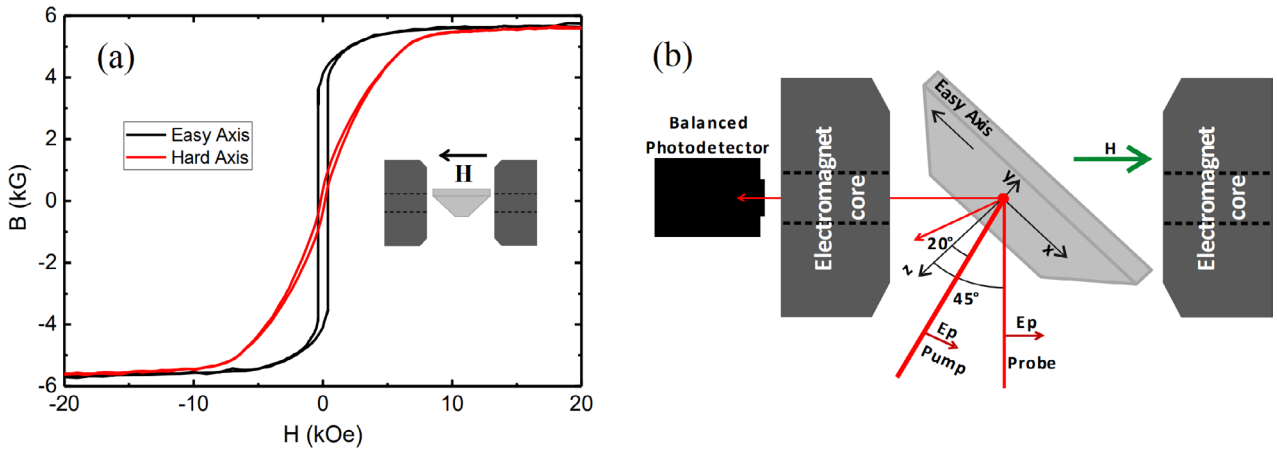

Figure 1. (a) In-plane magentization along 'easy' and 'hard' anisotropy axes; (b) magneto-optical pump-probe experimental schematic.

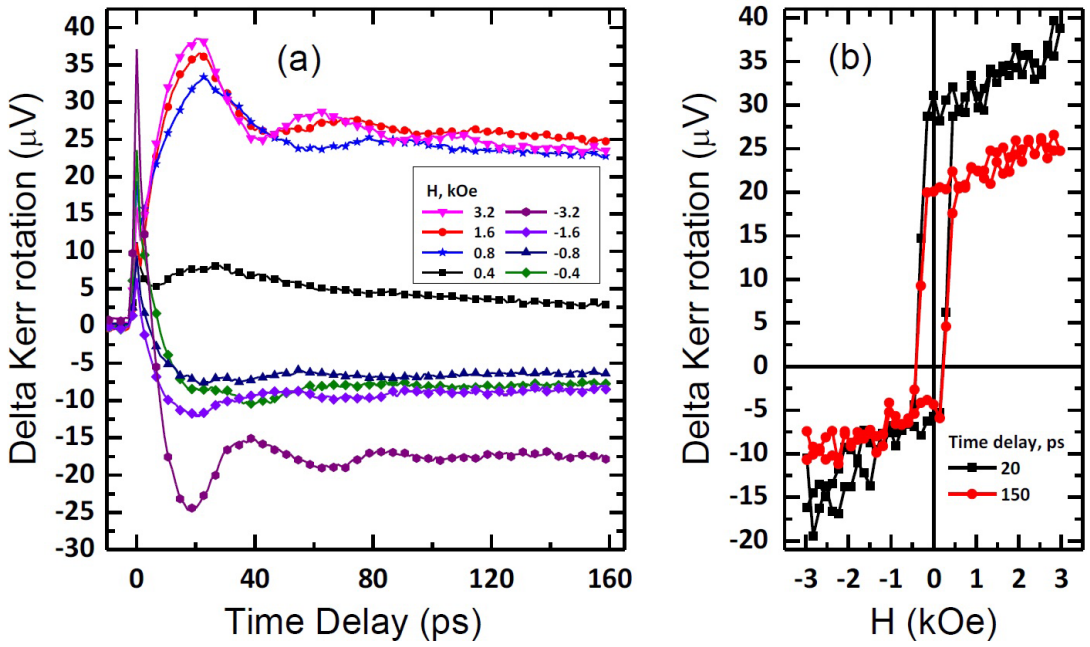

Figure 2. 'Easy axis' geometry. (a) Dependence of the Kerr rotation angle on the delay time for different values of magnetic field strength; (b) Kerr rotation hysteresis loops at maximum of the first oscillation ($t = 20$ ps) and after oscillations attenuation ($t = 150$ ps).

loop presented in figure 3 is not limiting but a partial one. The curves of relaxation of the polarization angle presented in figures 3(c) and (d) are also even regarding to the magnetic field sign and depend strongly on the direction of magnetic field variation (shown by arrows in figure 3(a)). Oscillations appear practically against the background of the zero signal; relaxation of oscillatory part of magneto-optical signal occurs on the same time scale that the total magneto-optical signal. For the maximal value of the rotation angle shown in the hysteresis loop in figure 3(a) as points M1 and M2, the temporal dependences are very unstable; data of the sequences of identical measurements in point M1 are shown in figure 3(b).

It is important to emphasize that the observed behavior possesses a threshold; oscillations appear only for the pump power over 0.85 mJ cm^{-2}.Change of the probe polarization from 'p' to 's' did not affect the results.

We can suggest a qualitative explanation for the observed phenomena as a result of pump-induced thermal effect on the anisotropy field. The origin of the uniaxial anisotropy in the structure under consideration is exchange interaction between rare-earth (TbCo2) and 3d (FeCo) layers [15]. One can suppose that a rapid increase of spin temperature of 3d electrons under an optical pump [19] should disrupt interlayer interaction and affect anisotropy induced by application of magnetic field during deposition of the multilayer structure. In the 'hard axis' geometry, the main feature of the photo-excitation of spin system is a symmetrical hysteretic loop presented in figure 3(a). This behavior of spin oscillations can be explained by symmetry of photo-induced torque T. Perturbation of the anisotropy field $\Delta H_a \frac{M_y}{M} \vec{y}$ generates two components of the torque: $T_z \propto -(M_x M_y)\Delta H_a$ and $T_x \propto (M_z M_y)\Delta H_a$. Dependence of T_z on the angle φ between hard axis and projection of magnetic moment on the sample plane is shown in figure 4(a). If positive magnetic field is of maximal value for the experimental conditions, then the angle φ is close to $\varphi/4$. When the magnetic field decreases, magnetization rotates

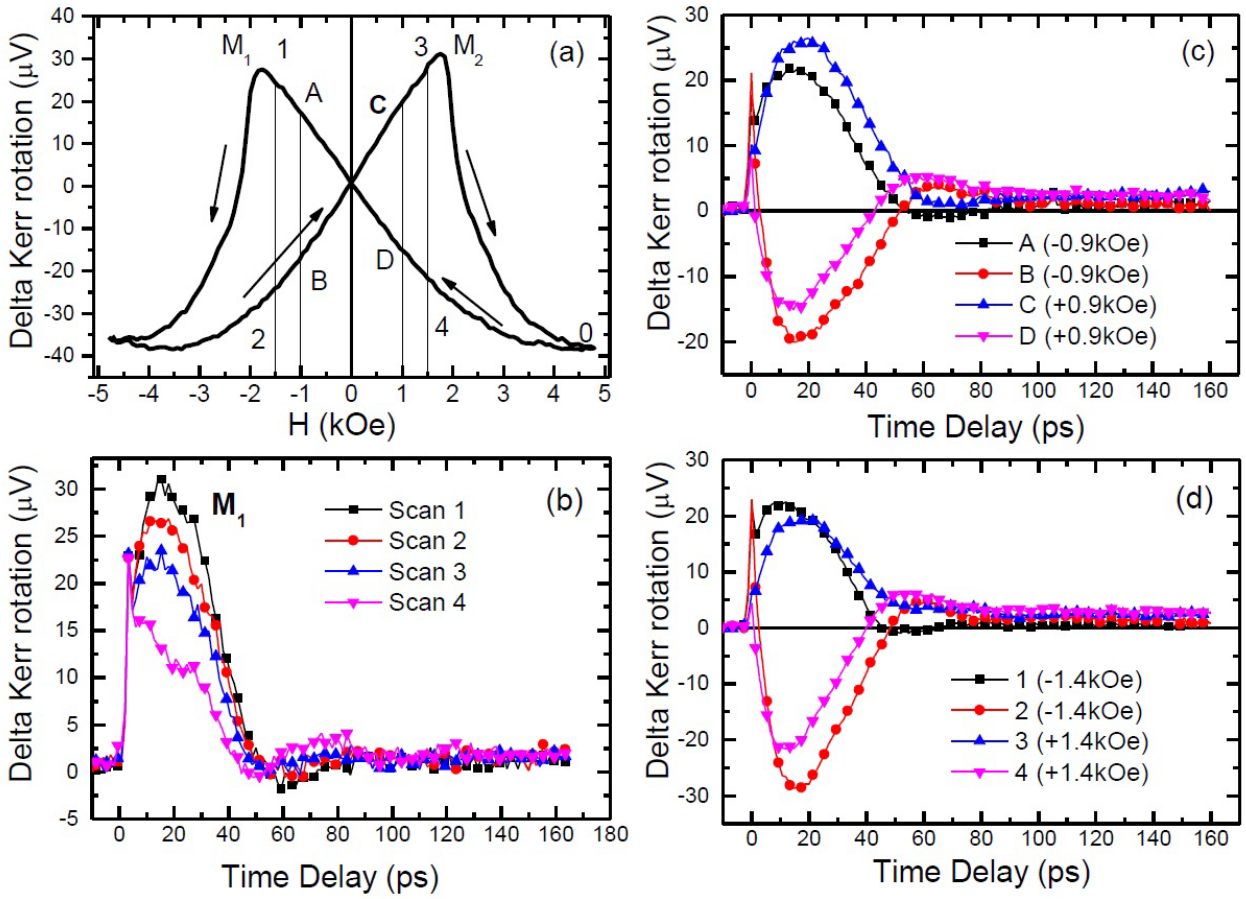

Figure 3. 'Hard axis' geometry. (a) Kerr rotation hysteresis loops at maximum of the first oscillation ($t = 20$ ps); dependences of the Kerr rotation on the delay time for different points on the Kerr hysteresis loop shown in the picture (a); instability in point M_1 is illustrated by consecutive identical scans (b); data measured in points A, B, C, D (c) and in points 1, 2, 3, 4 (d).

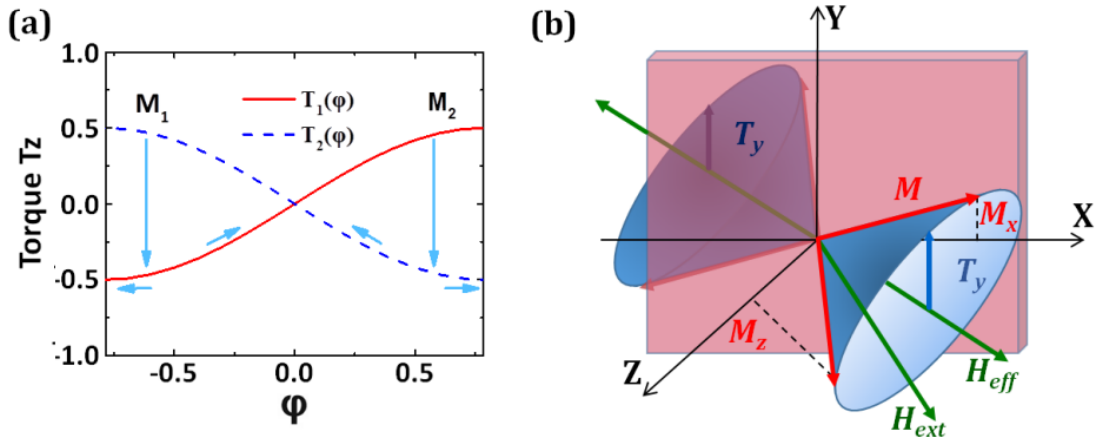

Figure 4. (a) Hysteretic dependence of the photo-induced torque T_z on angle φ between the 'hard axis' and projection of the magnetic moment on plane of the sample: M_1 and M_2 switching points from metastable to stable states. (b) Schematic presentation of the magnetic moment precession in opposite transitive effective field H_{eff}. The initial photo-induced projection M_y is even relatively to magnetizing field but direction of precession is odd.

towards the easy axis. The subsequent change of sign of the magnetic field changes the sign of projection M_x. For strict orientation of the magnetic field normally to the easy axis, two opposite projections M_y are energetically equivalent. But a small deviation (about 1°) of the field from the normal selects one preferable sign of M_y. Such an orientation corresponds to a stable state while the opposite orientation is metastable. These states are separated by an energy barrier. An orientation that is stable for one direction of magnetizing field becomes metastable for the opposite one. Projection of M_x reverses without change of sign of M_y if a negative magnetizing field is not too strong. Thus, the torque T_z changes the sign. When the field reaches its critical value, the projection M_y switches from metastable to stable state as it is illustrated in figure 4

(line $T_2(\varphi)$, point M_1). As a result, the signs of T_z for negative and positive magnetic field coincide. Further increase of negative field brings T_z to the initial value characteristic for the strongest positive field. Variation of the field strength in the opposite direction from negative to positive maximal value repeats the field dependence of T_z in mirror manner (line $T_1(\varphi)$ in figure 4), and forms a symmetric hysteretic loop. The torque projection T_z excites the normal component of the magnetic moment accompanied by the hysteretic polar Kerr effect. The similar behavior is expected for T_x projection that excites the longitudinal x-component of magnetization associated with the meridional Kerr effect. At the switching points M_1 and M_2 the magnetic system is unstable, which is reflected in the instability of the Kerr rotation observed experimentally. In real samples, the switch is not sharp because of a reversal of magnetization by the domain wall's motion.

In the 'easy axis' geometry, variation of the anisotropy field creates T_y component of the torque $T_y \propto (M_z M_x)\Delta H_a$ that is even relatively to the sign of the magnetizing field. It determines the same initial phase of the photo-excited precession. The same initial phase of y-projection (blue arrow) corresponds to change of sign for both x and z dynamic projections when the magnetic field is reversed (see figure 4(b)). These projections are responsible for the odd photo-induced meridional and polar Kerr effect, respectively.

4. Conclusion

The results of spin excitation studies in the 'hard axis' geometry reveal pump-induced disruption of the anisotropy field. Taking into account the origin of uniaxial anisotropy created in the heterostructure due to exchange coupling between rare-earth and 3d layers one can suppose an impact of the pump on the interlayer exchange. The feature of spin excitation in the 'easy axis' geometry is long time relaxation of the photo-induced transitive state of the magnetic system (analogously to the observed earlier in the in-plane magnetized FePt film [20] and CoFeB [21]). This feature can be also related to the method of creating the uniaxial anisotropy by application of a magnetic field during the process of deposition of the magnetic structure at room temperature. Thermal perturbation of the field induced stable electronic states can be qualitatively different when the magnetic field is applied in parallel or perpendicular directions. Microscopic analysis of the anisotropic relaxation of the transitive states is however out of the scope of this report. In conclusion, we note that the presented results point to ultrafast (less than 20 ps) optical control of field induced magnetic anisotropy in an intermetallic heterostructure that is of interest for applications as a mechanism of fast switching of magnetic states near SRT.

Acknowledgments

This work was supported by the Russian Foundation for Basic Research (Grant No. 18-52-16021). Participation of EDM is supported by the Ministry of Education and Science in the framework of government assignments to universities (FSFZ-2020-0022), and VLP in accordance with the program of the Presidium RAS No. 5 'Photonic technology in sensing of inhomogeneous media and bio-objects'.

ORCID iDs

Mikhail Gaponov https://orcid.org/0000-0003-0003-5054
Sergei Ovcharenko https://orcid.org/0000-0002-6360-3672
Nicolas Tiercelin https://orcid.org/0000-0001-7400-4272
Elena Mishina https://orcid.org/0000-0003-0387-5016
Vladimir Preobrazhensky https://orcid.org/0000-0002-6206-5948

References

[1] Li X, Kang A, Liu Z and Zhou Y 2019 *Appl. Phys. Lett.* **114** 012403
[2] Huisman T J *et al* 2016 *Nat. Nanotechnol.* **11** 455
[3] Wang S *et al* 2018 *Appl. Phys. Lett.* **113** 171108
[4] Lattery D M, Zhu J, Zhang D, Wang J P, Crowell P A and Wang X 2018 *Appl. Phys. Lett.* **113** 162405
[5] Afanasiev D, Ivanov B A, Pisarev R V, Kirilyuk A, Rasing T and Kimel A V 2017 *J. Phys.: Condens. Matter* **29** 224003
[6] De Jong J A, Kimel A V, Pisarev R V, Kirilyuk A and Rasing T 2011 *Phys. Rev.* B **84** 104421
[7] De Jong J A, Kalashnikova A M, Pisarev R V, Balbashov A M, Kimel A V, Kirilyuk A and Rasing T 2017 *J. Phys.: Condens. Matter* **29** 164004
[8] Le Guyader L, Kleibert A, Nolting F, Joly L, Derlet P M, Pisarev R V, Kirilyuk A, Rasing T and Kimel A V 2013 *Phys. Rev.* B **87** 054437
[9] Tang J, Ke Y, He W, Zhang X, Zhang W, Li N, Zhang Y, Li Y and Cheng Z 2018 *Adv. Mater.* **30** 1706439
[10] Peng B *et al* 2017 *ACS Nano* **11** 4337
[11] Klimov A, Tiercelin N, Dusch Y, Giordano S, Mathurin T, Pernod P, Preobrazhensky V, Churbanov A and Nikitov S 2017 *Appl. Phys. Lett.* **110** 222401
[12] Tiercelin N, Dusch Y, Giordano S, Klimov A, Preobrazhensky V and Pernod P 2016 *Nanomagnetic and Spintronic Devices for Energy-Efficient Memory and Computing* (New York: Wiley) ch 8 pp 221–57
[13] Mathurin T, Giordano S, Dusch Y, Tiercelin N, Pernod P and Preobrazhensky V 2016 *Appl. Phys. Lett.* **108** 082401
[14] Ilyin N A, Klimov A A, Tiercelin N, Pernod P, Mishina E D, Gaponov M S, Brekhov K A, Sigov A S and Preobrazhensky V L 2018 *Russ. Technol. J.* **3** 50
[15] Klimov A *et al* 2006 *IEEE Trans. Magn.* **42** 3090
[16] Hohlfeld J, Matthias E, Knorren R and Bennemann K H 1997 *Phys. Rev. Lett.* **78** 4861
[17] Tiercelin N, Ben Youssef J, Preobrazhensky V, Pernod P and Le Gall H 2002 *J. Magn. Magn. Mater.* **249** 519
[18] Schwieger S, Kienert J and Nolting W 2005 *Phys. Rev.* B **71** 024428
[19] Li W, Yan J, Tang M, Lou S, Zhang Z, Zhang X L and Jin Q Y 2018 *Phys. Rev.* B **97** 184432
[20] Chen Z, Yi M, Chen M, Li S, Zhou S and Lai T 2012 *Appl. Phys. Lett.* **101** 222402
[21] Liu B, Ruan X, Wu Z, Tu H, Du J, Wu J, Lu X, He L, Zhang R and Xu Y 2016 *Appl. Phys. Lett.* **109** 042401